General Disclaimer

- This document has been reproduced from the best copy furnished by the organizational source. It is being released in the interest of making available as much information as possible.

- This document may contain data, which exceeds the sheet parameters. It was furnished in this condition by the organizational source and is the best copy available.

- This document may contain tone-on-tone or color graphs, charts and/or pictures, which have been reproduced in black and white.

- This document is paginated as submitted by the original source.

- Portions of this document are not fully legible due to the historical nature of some of the material. However, it is the best reproduction available from the original submission.

NASA

Technical Memorandum 86173

The Galactic Gamma-Ray Distribution: Implications for Galactic Structure and the Radial Cosmic Ray Gradient

A. K. Harding and F. W. Stecker

NOVEMBER 1984

National Aeronautics and
Space Administration

Goddard Space Flight Center
Greenbelt, Maryland 20771

THE GALACTIC GAMMA-RAY DISTRIBUTION: IMPLICATIONS FOR GALACTIC STRUCTURE AND THE RADIAL COSMIC RAY GRADIENT

A. K. Harding and F. W. Stecker

Laboratory for High Energy Astrophysics

NASA Goddard Space Flight Center

ABSTRACT

We have derived the radial distribution of gamma-ray emissivity in the Galaxy from flux longitude profiles, using both the final SAS-2 results and the recently corrected COS-B results and analyzing the northern and southern galactic regions separately. We have then made use of the recent CO surveys of the southern hemisphere, in conjunction with the northern hemisphere CO data, to derive the radial distribution of cosmic rays on both sides of the galactic plane. We have found that, in addition to the "5 kpc ring" of enhanced emission, there is evidence from the asymmetry in the radial distributions for spiral features which are consistent with those derived from the distribution of bright HII regions. We find positive evidence for a strong increase in the cosmic ray flux in the inner Galaxy, particularly in the 5 kpc region, in both halves of the plane.

I. INTRODUCTION

It has long been recognized that γ-ray astronomy provides a powerful tool for studying the origin and distribution of the primary cosmic radiation (Ginzburg and Syrovatsky 1964; Fazio 1967) and also for revealing the structure of the Galaxy (Stecker 1971, 1977, 1978). An important feature of large scale galactic structure was obtained quite early from analysis of the preliminary SAS-2 data when it was deduced that the γ-ray emissivity of the Galaxy has a large maximum in a ring at about 5 kpc from the galactic center (Stecker, et al. 1974) and this feature was then quickly related to a newly discovered 5 kpc ring of giant molecular clouds in the Galaxy (Solomon and Stecker 1974, Scoville and Solomon 1975, Stecker et al. 1975).

Because the Galaxy is transparent to γ-rays, γ-ray surveys can be used in conjunction with galactic surveys at other wavelengths to provide a "synoptic" approach to the general problem of galactic structure (Stecker 1981). There have been basically two distinct approaches for theoretical research on this problem. One approach, which can be called the "modeling approach", is to adopt a model for galactic spiral structure based on observations at more traditional astronomical wavelengths, to then make an assumption relating the cosmic ray and gas distributions, and to check for consistency between the γ-ray distribution implied by the model and the actual observations. This approach has been used extensively by Fichtel, Kniffen and coworkers (e.g., Fichtel and Kniffen 1984).

The other approach is to start with the γ-ray observations themselves, and to use them together with information gathered at other wavelengths to deduce new information about galactic structure and the galactic cosmic ray distribution by employing geometrical unfolding and analysis techniques (Puget and Stecker 1974, Solomon and Stecker 1974, Stecker 1975, Strong 1975, Stecker

1977, Caraveo and Paul 1979). In this approach, a key element has been the understanding that molecular hydrogen plays an important role in the problem (Stecker 1969, Stecher and Stecker 1970). Because of this fact, applications of the unfolding approach have been limited by the lack of information on the distribution of molecular hydrogen on the southern hemisphere side of the galactic disk. This lack has now been remedied as the results of recent southern hemisphere survey are now becoming available (Sanders, Solomon and Scoville 1984; Robinson et. al. 1984). In this paper, we make use of these new results, as well as the final SAS-2 γ-ray survey data, and the COS-B γ-ray survey results, newly corrected for intrinsic background, in order to reexamine the galactic structure and galactic cosmic-ray gradient problems.

II. GAMMA-RAY FLUX UNFOLDING METHOD

Observations of the galactic gamma-ray emission in the form of flux-longitude profiles give the total integrated emission along a line of sight. Several methods have been used to unfold the flux-longitude profiles and derive the gamma-ray emissivity as a function of galactic coordinates, $Q(R,\theta)$, making a necessary assumption about the symmetry of $Q(R,\theta)$. Strong (1975), Strong and Worrall (1976) and Caraveo and Paul (1979) used a numerical matrix inversion to unfold the SAS-2 data, assuming either cylindrically symmetric or spiral arm models for Q. Puget and Stecker (1974) derived an analytic expression for the unfolded radial gamma-ray emissivity distribution, assuming cylindrical symmetry. They then proceeded to a numerical analysis using the earliest SAS-2 data. We will use this latter method to unfold the most recently published results from both the SAS-2 and COS-B satellite detector experiments.

We assume cylindrical symmetry in each half of the galactic plane so that

$Q(R,\theta) = Q(R)$ is a function only of galactocentric radius R, and is independent of distance z above the galactic plane up to a height, h. The gamma-ray flux, $I(\ell)$, in photons $cm^{-2}\ s^{-1}\ rad^{-1}$ can be written,

$$I(\ell) = \frac{R_\odot}{2\pi} \int_0^{b_m} db \int_0^{(h/R_\odot)\cot b} d\rho\ Q(r) \qquad (1)$$

where R_0 is the galactocentric distance of the Sun, ρ is heliocentric distance, $r = R/R_\odot$ and b is galactic latitude. We divide $I(\ell)$ into flux contributions from the inner ($r < r_0$) and outer ($r > r_0$) parts of the Galaxy, $I = I_1 + I_0$, and assume that the emissivity in the outer Galaxy, $Q_0(R)$, is constant for $r_0 < r < r_m$. Using Eq (1) and $\rho = \cos\ell + (r^2 - \sin^2\ell)^{1/2}$, we find the following expression for the outer galaxy flux component

$$I_0(\ell) = \frac{Q_0 h}{2\pi} \ell n \left(\frac{\rho_m}{\rho_0^+}\right) + \frac{R_\odot Q_0}{2\pi} \rho_0^- \cot^{-1}\left(\frac{R_\odot \rho_0^-}{h}\right) + \frac{Q_0 h}{4\pi} \ell n\left\{\left[1 + \left(\frac{R_\odot \rho_0^-}{h}\right)^2 \sin^2 b_m\right]\right\}$$

where, (2)

$$\rho_m = \cos\ell - (r_m^2 - \sin^2\ell)^{1/2}$$

$$\rho_0^{\pm} = \cos\ell \pm (r_0^2 - \sin^2\ell)^{1/2}$$

Using this expression, we can determine the part of the observed flux from emission at galactic radii less than r_0 and invert this flux to find the inner Galaxy emissivity $Q_1(r)$. Using Eq (1), the inner galaxy flux may be written,

$$I_i(\ell) = \frac{h \cos \ell}{2\pi} \int_{\sin^2 \ell}^{r_m^2} dr^2 \frac{Q_i(r)}{(1-r^2)(r^2-\sin^2\ell)^{1/2}} \qquad (3)$$

Puget and Stecker (1974) have shown that this equation can be inverted with the use of Laplace transforms to give the following solution for $Q_i(r)$,

$$Q_i(r) = \frac{2(1-r^2)}{h} \int_{r^2}^{r_m^2} dn\, (n-r^2)^{-1/2} \frac{d}{dn} \left[-\frac{I_i(\ell)}{\cos\ell}\right] \qquad (4)$$

where $n = \sin^2\ell$. The $\cos\ell$ in the denominator of the integrand accentuates local fluctuations in the flux ($\ell \sim 90°$ and $\ell \sim 270°$) which can overpower the flux derivatives in more distant regions. Since we are mainly interested here in the large-scale distribution of gamma-ray emissivity in the Galaxy, we can eliminate these fluctuations in the unfolding due to local sources of emission by taking $r_0 = 0.85$, which corresponds to longitudes $300° \lesssim \ell \lesssim 60°$.

We have used this technique to unfold both SAS-2 and COS-B longitude data. The SAS-2 data for energies > 100 MeV from Hartman et. al (1979) is integrated over latitudes $|b| \leq 10°$ and has a longitude resolution of 2.5°. Mayer-Hasselwander (1983) has presented a COS-B longitude profile for energies > 100 MeV with a longitude resolution of 2.5° for direct comparison with the SAS-2 profile. With a COS-B background subtraction of 8×10^{-5} ph cm^{-2} s^{-1} sr^{-1} above 70 MeV, the two data sets were found to be in agreement within the statistical errors at most longitudes. It was also found that the COS-B flux must be multiplied by a factor of 1.17 to bring the general flux levels of the two data sets into agreement. In addition to this COS-B data set, we have unfolded the COS-B data in the energy range 0.3 - 5 GeV from Mayer-Hasselwander et. al. (1982), which were also averaged over $|b| \leq 10°$ but have a longitude resolution of 1°.

An outer galaxy flux contribution is determined from Eq (2), assuming a

constant value $Q_0 = 1.1 \times 10^{-25}$ cm^{-3} s^{-1} ($E > 100$ MeV) and $Q_0 = 0.51 \times 10^{-25}$ cm^{-3} s^{-1} ($.3 < E < 5$ GeV) and constant scale height $h = 150$ pc between $r_0 = 0$ .85 and $r_m = 1.4$. The value of $Q_0 = q_0 \langle n_H \rangle$ was derived from a local gamma-ray production rate $q_0 = 1.9 \times 10^{-25}$ s^{-1} for $E > 100$ MeV (Stecker 1977, Fichtel and Kniffen 1984) and $q_0 = 8.8 \times 10^{-26}$ s^{-1} for $0.3 < E < 5$ GeV, taking a local average H-atom density of $\langle n_H \rangle = 0.6$ cm^{-3}. This outer galaxy emissivity gives approximately the flux levels observed in the anticenter directions. Our adopted values for q_0 agree with those recently derived by Bloemen et al. (1984) to within ~ 15%. They obtain q_0 (>100 MeV) = 2.2×10^{-25} s^{-1} (extrapolating from a lower energy of 70 MeV) and q_0 (0.3-5 GeV) = 7.4×10^{-25} s^{-1}.

Before unfolding, the flux data points were first averaged over a longitude range of 7.5° in the case of the > 100 MeV data and 7° in the case of the high energy COS-B data in order to smooth out fluctuations. The outer galaxy flux contribution, determined by the method described above, was subtracted from the total flux at each longitude to obtain an inner galaxy flux contribution. The derivatives $d/dn(-I_i/\cos\ell)$ in Eq (4) were then evaluated from a cubic spline fit to the averaged flux data points in the longitude range $300° < \ell < 60°$ from which the outer galaxy flux as determined above was subtracted.

Errors in the calculated emissivities were estimated by assuming that the standard deviations of the derivatives, which would be difficult to determine exactly from the spline fits which correlate all the points and their errors, are just equal to those of the fluxes at those points. Propagating these errors in Eq (4) then gives error values for each of the derived emissivities. In order to confirm that reasonable estimates have been made for the errors, we have obtained the expected statistical spread in the

emissivity profiles for several cases by computing different realizations of the profiles from a Monte Carlo sampling of the observed flux errors. The variation in the profiles was found to agree quite well with the error propagation method, which gives the actual error values and thus enables us to plot error bars on the emissivity profiles. We note, however, that because of the correlations introduced by the spline fits, the errors in adjacent Q(r) values are strongly correlated and thus the error bars do not represent independent errors.

III. RADIAL EMISSIVITY DISTRIBUTIONS

Results from unfolding the three flux-longitude profiles described in Section II are shown in Figures 1 - 3. The radial distributions of gamma-ray emissivity (times scale height) for the SAS-2 and COS-B data at energies > 100 MeV are plotted in Fig. 1. The appearance of negative emissivities in several regions, the only significant one being the 1.5 - 3.5 kpc region in the South, results from a breakdown in the assumption of cylindrical symmetry. Strong or local points sources and spiral structure could be responsible for such departures from cylindrical symmetry. Both of these features are probably present in the data. There is general agreement in the shapes of the COS-B and SAS-2 emissivity distributions, the dominant features being a peak between 5 and 6 kpc in the North and a peak between 4 and 5 kpc in the South, which seem to describe an asymmetric ring of emission. The emission appears to be most intense on the inner rim. There is also a maximum emissivity near the Galactic center and a secondary peak of emission around 7.5 kpc in the South, which is more pronounced in the COS-B data. The position and magnitude of the peak near the galactic center are uncorrected for significant contributions from local emission near $\ell=0°$ in the latitude range $|b|<10°$.

(For a more precise treatment of galactic center emission, see Blitz, Bloemen and Hermsen, 1984).

A general construction of the galactic emission map is shown in Fig. 3. The COS-B emissivity levels in the 5 kpc region are significantly less than those of SAS-2 relative to the same local emissivity. There are several factors which influence the peak-to-local emissivity ratios in the unfolding process. A higher outer galaxy emissivity level would decrease the peak-to-local ratio, but it would do so by the same factor in both sets of data. If a higher background level were subtracted from the COS-B longitude flux prior to unfolding, the peak to local emissivity would increase, bringing it into better agreement with the results for the SAS-2 flux, which had essentially no background. Figure 2 shows the radial emissivity distribution obtained from the COS-B flux after first subtracting a small additional 0.2×10^{-4} cm^{-2} s^{-1} sr^{-1} intrinsic instrumental background correction (using 0.15×10^{-4} produced similar results). Recent reanalysis of the COS-B detector background has indicated that such a higher background correction level of this order may be justified, although the precise amount of this correction is still uncertain (Mayer-Hasselwander, private communication). Within the errors, this emissivity distribution now agrees with the SAS-2 emissivity, but the peak-to-local ratios are still lower in both the North and South.

Our results on the COS-B radial distribution of > 100 MeV gamma-rays (without additional background subtraction) give an emissivity in the 5 kpc ring which is 4-5 times the local value. This is significantly larger than the ratio of 2-3 obtained by Mayer-Hasselwander (1983) from an unfolding of the same data set. The discrepancy may be explained by the fact that our assumed value of $\langle n_H \rangle = 0.6$ cm^{-3} (Burton 1976), is lower than his assumed value of 1 cm^{-3}. Our resulting value for the local emissivity is about half

as much, producing a higher contrast to the emissivity in the 5 kpc region. In addition to changing the normalization of the radial distribution, a lower local emissivity gives a smaller flux contribution from the outer galaxy and therefore a larger remaining flux contribution from the inner galaxy. We were in fact able to reproduce the results of Mayer-Hasselwander's unfolding by taking our local emissivity to be twice the value given in Section II.

Figure 4 shows the results of unfolding the COS-B flux data in the highest energy range, $0.3 < E < 5$ GeV. The emissivity profile looks much the same as at lower energies, however the errors here are somewhat larger. The level of negative emissivity around 2 kpc in the South is not as large as at lower energies, even though the flux data has been averaged over a slightly smaller longitude range before unfolding. This may be an indication that the negative emissivities result in part from local fluctuations or sources, since the high energy data, being more confined to the plane (Mayer-Hasselwander et. al. 1982), is relatively less sensitive to local effects.

IV. COSMIC RAY DISTRIBUTION

The results presented in the previous section give distributions of the total observed gamma-ray emissivity in the Galaxy. This emission has two basic types of component: 1) diffuse emission from cosmic rays interacting with gas or with a low energy radiation background, and 2) point source emission from pulsars, accreting compact objects, etc. The total point source contribution is uncertain, but estimates of the emission level from pulsars (Harding 1981, Harding and Stecker 1981, Salvati and Massaro 1982) are in the range 15% - 20% or less. We note that pulsars are the only true galactic gamma-ray point sources known, even though there exist 30 or so "point sources" with angular sizes of 1° - 2° in the COS-B catalog (Swanenburg et.

al. 1981), many of which could be diffuse. At least 80% - 90% of the emissivity at low latitudes, where the Compton component is low (Kniffen and Fichtel 1981), can then be presumed to result from interactions between cosmic rays and gas in the form of molecular and atomic hydrogen. In addition, the galactic point source emission may be distributed like the diffuse emission (Harding and Stecker 1981) so that its effect does not distort the overall flux distribution. Therefore, information on the distribution of gas in the Galaxy can be used in conjunction with the observed gamma-ray emissivity to yield information on the galactic cosmic ray distribution (e.g. Stecker and Jones 1977).

The quantity, q_γ, the gamma-ray emissivity per H-atom, is derived from the observed gamma-ray volume emissivity, total gas density, n_{TOT}, and gas scale height, h_G, by the following:

$$q_\gamma (r) = \frac{Q_\gamma(r)h}{n_{TOT}\, h_G} \tag{5}$$

The total gas density is the sum of molecular, n_{H_2}, and atomic, n_{HI}, densities, $n_{TOT} = 2\, n_{H_2} + n_{HI}$. Molecular hydrogen densities have been derived from galactic CO surveys which have recently been extended to include southern galactic longitudes. Longitude-velocity data from these surveys can be unfolded using a galactic rotation curve to give CO radial emissivity distributions, which can then be converted to molecular hydrogen densities. We use here the recent CO survey results of Robinson et. al. (1984), who give radial distributions of J (K km s^{-1} kpc^{-1}) in the ^{12}CO (1-0) transition for both the North and South, and scale heights as a function of galactic radius. The radial CO distribution shows the bulk of emission concentrated in a ring of radius ~ 5 kpc, with the emission in the South distributed in a

broad peak between 2.5 and 8.5 kpc, in contrast to the sharp peak in the North at 5 kpc. Using their conversion factor, $n_{H_2} = 0.12\ J\ (CO^{12})\ \ cm^{-3}$, we computed the molecular gas densities in 1 kpc radial bins, and then added a constant atomic hydrogen density of 0.35 cm^{-3} for R > 4 kpc. A combined scale height was obtained for each radial bin as a weighted average of the molecular scale heights and a constant HI scale height of 250 pc. The values for h_G calculated in this way increase by at least a factor of two between R = 2 kpc and R = 10 kpc due to both an increasing CO scale height and an increasing fraction of atomic gas, which has a much larger scale height than the CO.

Figure 5 shows the radial distribution of $q_\gamma(\ >\ 100$ MeV) derived using the SAS-2 and COS-B emissivities plotted in Fig. 1. If all the gamma-ray emissivity were from diffuse processes, then q_γ would be proportional to the density of cosmic rays. The emissivity per H-atom derived from both the SAS-2 and COS-B data show evidence for an increase in the inner galaxy relative to local values in both the North and the South. The COS-B gradient, however, is significantly smaller than the SAS-2 gradient due to smaller COS-B emissivities in the inner Galaxy. In fact the value of q_γ is less than the local value over a number of bins, which would require a decrease in cosmic ray density to compensate for a gradient in gas density steeper than the gamma-ray emissivity gradient. Figure 6 shows the distribution of q_γ using the COS-B emissivity for the case of a higher background subtraction (cf. Fig. 2), which increases the gamma-ray volume emissivity gradient and thus the implied cosmic ray gradient, bringing it into agreement (within the errors) with the SAS-2 result.

We can also compare the gamma-ray emissivity per H-atom for the COS-B data in the two energy ranges E > 100 MeV and 0.3 < E < 5 GeV. Since diffuse processes involving cosmic-ray protons produce different gamma-ray spectra than those processes involving electrons, variations in the cosmic-ray

gradient as a function of energy would reveal differences in the distribution of cosmic-ray protons and electrons as suggested by Bloemen, et al. (1984) for the outer Galaxy. In the 0.3 - 5 GeV energy range the distribution of q_γ plotted in Fig. 7 shows no statistically significant variation from the lower energy distribution plotted in Fig. 5, indicating that, at least in the inner Galaxy, cosmic-ray protons and electrons probably have the same radial distribution.

V. DISCUSSION OF RESULTS

Our results generally confirm the phonomenology of the 5 kpc "Great Galactic Ring" and cosmic ray gradient derived earlier using the northern hemisphere data (Stecker, et al. 1975, Stecker 1977) and extend the ring phenomenology to the southern hemisphere region of the Milky Way. In addition, the southern galactic region gives evidence of more structure than the northern region does. This is true for the CO data, the γ-ray data, and the radio data on the distribution of HII regions and pulsars in the inner galaxy. In particular, the southern region gives evidence of enhanced γ-ray emission at a radial distance of 7 to 8 kpc from the galactic center (noted previously by Stecker 1977 and Caraveo and Paul 1979). Such emission is more evident in the COS B data than the SAS-2 data. This emission region represents only a small fraction of the emission coming from the 5-kpc ring. An interpolation of the northern and southern emissivity data as given in Fig. 3 leads most naturally to the interpretation that the emission is associated with a spiral arm feature of the Galaxy, the Carina arm. The overall emissivity pattern shown in Fig. 3 is consistent with the spiral pattern suggested by Georgelin and Georgelin (1976) based on the distribution of HII regions. The main γ-ray emission appears to lie in a region inside the spiral

pattern of the largest giant molecular clouds derived by Thaddeus and co-workers (to be published). All of these indications support the thesis that the galactic γ-ray emission is associated with the youngest regions of star formation in the Galaxy (Stecker 1976).

The existence of the 5 kpc ring of molecular clouds and associated stellar activity now appears to be beyond question. Molecular rings have also been seen in CO observations of a number of spiral galaxies (Young and Scoville 1982 and references therein.) Young and Scoville (1982) attribute their origin to exhaustion of gas by star formation in the nuclear bulge of spiral galaxies. It is interesting to note that prominent ring structures on a galactic scale are also produced in numerical simulations of the evolution of barred spiral galaxies. Such rings form at the ends of the bar and may be theoretically associated with the corotation radius (Schwarz 1984).

It is thus apparent that unfoldings of the γ-ray data have provided us with important clues as to the nature and structure of the Galaxy, independent of models based on data in other wavelength ranges. It is equally true, however, that data obtained from radio and infrared surveys which reveal the overall distribution of gas and dust in the Galaxy can be used in conjunction with the γ-ray data to derive a more complete synoptic picture (Stecker 1981). In particular, we find here that the $E_\gamma > 100$ MeV data reveal evidence of a cosmic-ray gradient in the inner Galaxy on both the northern and southern hemisphere sides of the galactic disk. We find some evidence of this also in the highest energy COS-B data, which has the best angular resolution, and which also may be the only region of the spectrum clearly dominated by pion decay γ-rays (Stecker 1977). These highest energy data have taken on additional importance with the claim of Bloemen, et al. (1984) that there may be no gradient in the nucleonic component in the outer Galaxy (a claim which, if true, would pose serious theoretical problems).

The cosmic-ray gradient derived for both the northern and southern galactic hemispheres also appears to peak in the region of the Great Galactic Ring where the supernova and pulsar distributions also have a maximum. This may most naturally argue for a galactic origin of the bulk of the nucleonic cosmic γ-rays, which have energies in the 1-10 GeV range. It has, of course, been realized for a long time that the cosmic ray electron component must be of galactic origin (Fazio, Stecker and Wright 1966).

We therefore feel that the existence of a radial gradient in the galactic cosmic ray distribution is now on firm ground. In fact, there is evidence that (owing to increased stellar nucleosynthesis) the ratio of CO to H_2 abundance may increase toward the galactic center, perhaps by up to a factor of 2 in the 5-6 kpc ring (Shaver, et al. 1983). This would reduce estimates of the average H_2 volume density in the inner Galaxy and would actually increase the derived gradient in the cosmic-ray flux by a corresponding factor. Such as increase would not qualitatively change our conclusions and would strengthen the argument for a general galactic cosmic-ray gradient.

REFERENCES

Blitz, L., Bleomen, J. B. G. M., and Hermsen, W. 1984, Astron. Ap., in press.

Bloemen, J. B. G. M., et al. 1984, Astron. Ap. 135, 12.

Burton, W. B., 1976, Ann. Rev. Astr. Ap. 14, 275.

Caraveo, P. A. and Paul, J. A. 1979, Astron. Ap., 75, 340.

Fazio, G. G., 1967, Ann. Rev. Astr. Ap., 5, 481.

Fazio, G. G., Stecker, F. W. and Wright J. P. 1966, Ap. J., 144, 611.

Fichtel, C. E. and Kniffen, D. A. 1984, Astron. Ap., 134, 13.

Georgelin, Y. M. and Georgelin, Y. P. 1976, Astron. Ap. 49, 57.

Ginzburg, V. L., and Syrovatsky, S. I. 1964, The Origin of Cosmic Rays (Oxford: Pergamon).

Harding, A. K. 1981, Ap. J., 247, 639.

Harding, A. K. and Stecker, F. W. 1981, Nature, 290, 316.

Hartman, R. C., Kniffen, D. A., Thompson, D. J., Fichtel, C. E., Ogelman, H. B., Tümer, T. and Özel, M. E. 1979, Ap. J., 230, 597.

Kniffen, D. A. and Fichtel, C. E. 1981, Ap. J., 250, 389.

Mayer-Hasselwander 1983, Space Sci. Rev., 36, 223.

Mayer-Hasselwander et. al. 1982, Astron. Ap., 105, 164.

Puget, J. L. and Stecker, F. W. 1974, Ap. J., 191, 323.

Robinson, B. J., Manchester, R. N., Whiteoak, J. B., Sanders, D. B., Scoville, N. Z. and Clemens, D. P. 1984, Ap. J. (Letters), 283, L31.

Salvati, M. and Massaro, E. 1982, M.N.R.A.S., 198, 11.

Sanders, D. B., Solomon, P. M. and Scoville, N. Z. 1984, Ap. J., 276, 182.

Schwarz, M. P. 1984, M.N.R.A.S. 209, 93.

Scoville, N. Z. and Solomon, P. M. 1975, Ap.J. 199, L105.

Shaver, P. A., McGee, R. X., Newton, L. M., Danks, A. C. and Pottasch, S. R. 1983, M.N.R.A.S. 204, 53.

Solomon, P. M. and Stecker, F. W. 1974, Proc. ESLAB Gamma-Ray Symposium, Frascati (ESRO SP-106), p. 253.

Stecker, F. W. 1969, Nature 222, 865.

Stecker, F. W. 1971, Cosmic Gamma Rays (Baltimore: Mono Book Corp.).

Stecker, F. W. 1975, Phys. Rev. Lett., 35, 188.

Stecker, F. W. 1976, Nature 260, 412.

Stecker, F. W. 1977, Ap. J., 212, 60.

Stecker, F. W. 1978, American Scientist, 66, 570

Stecker, F. W. 1981, Proc. Greenbank Workshop on The Phases of the Interstellar Medium (Greenbank, N.R.A.O.) ed. J. Dickey, p. 151.

Stecker, F. W. and Jones, F. C. 1977, Ap. J. 217, 843.

Stecker, F. W., Puget, J. L., Strong, A. W. and Bredekamp, J. H. 1974, Ap. J., 188, L59.

Stecker, F. W. , Solomon, P. M., Scoville, N. Z., and Ryter, C. E. 1975, Ap. J., 201, 90.

Strong, A. W. 1975, J. Phys., A8, 617.

Strong, A. W. and Worrall, D. 1976, J. Phys. A, 9, 823.

Thaddeus, P. and Dame, T. M. 1984, Occasional Rpts. Royal Soc. Edinborough, 13, 15.

Swanenburg et. al. 1981, Ap. J., 243, L69.

Young, J. S. and Scoville, N. Z. 1982, Ap.J., 260, L41.

FIGURE CAPTIONS

Fig. 1. Gamma-ray surface emissivity (volume emissivity times scale height) as a function of galactocentric radius in units of R_0 = 10 kpc, derived from the SAS-2 and COS-B data at energies greater than 100 MeV. The right hand scale shows the emissivities relative to the local value.

Fig. 2. Gamma-ray surface emissivity distribution derived from the COS-B data at energies greater than 100 MeV with an additional background subtraction (see text).

Fig. 3. Schematic map of the γ-ray emissivity in the inner Galaxy looking down on the galactic plane, constructed from the radial distributions shown in Fig. 1, omitting the galactic center region. The positions of the Sun and the galactic center are indicated by the appropriate symbols.

Fig. 4. Gamma-ray surface emissivity distribution derived from the COS-B data in the high energy (0.3 - 5 GeV) channel.

Fig. 5. Radial distribution of γ-ray emissivity per H atom above 100 MeV in the Northern and Southern halves of the Galaxy derived from the radial surface emissivity distributions shown in Fig. 1 using the CO data of Robinson, et al (1984).

Fig. 6. Emissivity per H atom as in Fig. 5, but using an extra background subtraction to the COS-B data (see text). The results are compared with those obtained from the SAS-2 data.

Fig. 7. Gamma-ray emissivity per H atom derived from the COS-B radial surface emissivity distribution in the high energy channel (0.3 - 5 GeV) shown in Fig. 4.

Fig. 1

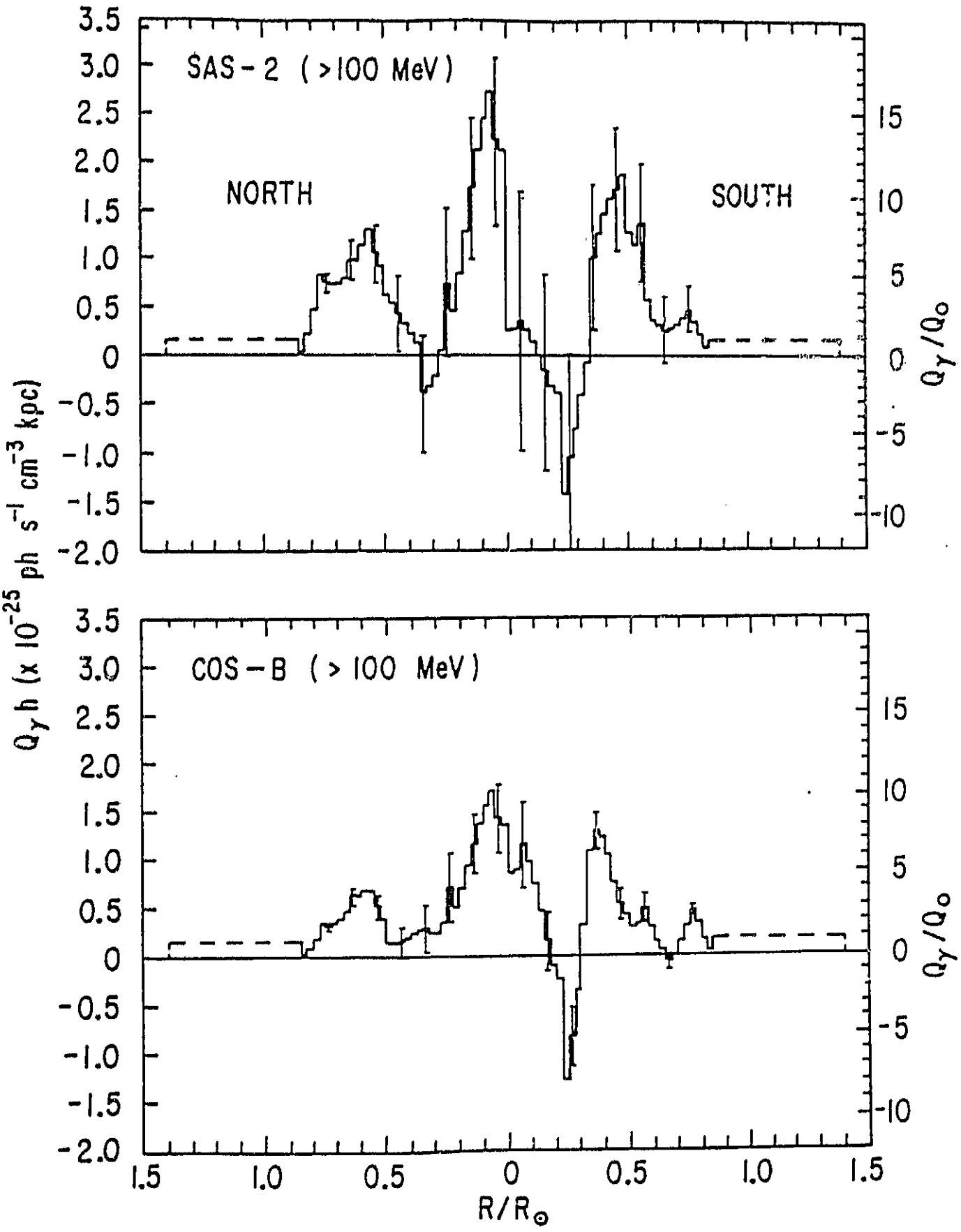
SAS-2 (>100 MeV)
NORTH
SOUTH
COS-B (>100 MeV)
$Q_\gamma h$ (x 10^{-25} ph s^{-1} cm^{-3} kpc)
Q_γ/Q_o
$R/R_\odot$
3.5
3.0
2.5
2.0
1.5
1.0
0.5
0
-0.5
-1.0
-1.5
-2.0
15
10
5
0
-5
-10
1.5
1.0
0.5
0
0.5
1.0
1.5

Fig. 2

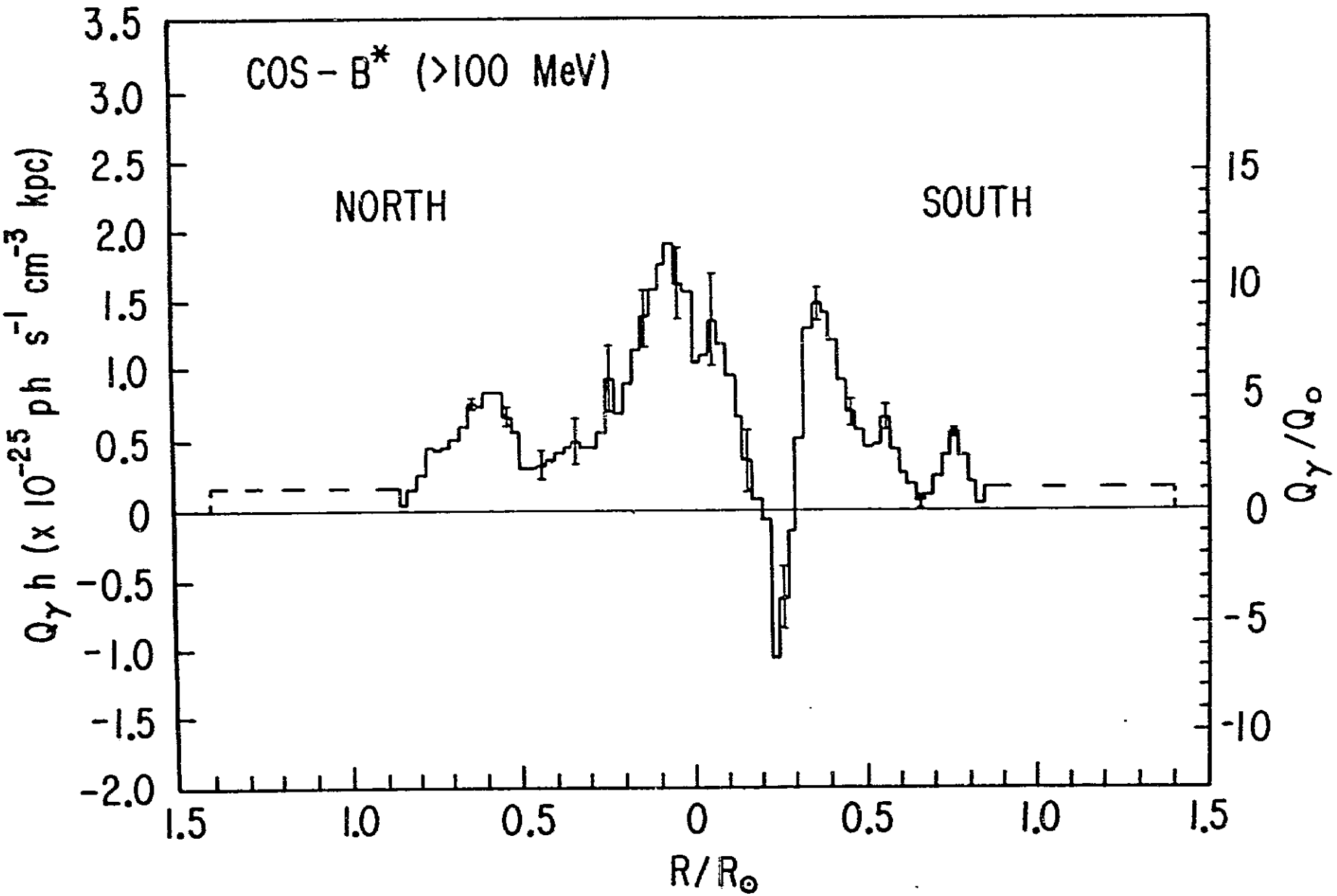
COS - B* (>100 MeV)
NORTH
SOUTH
$Q_\gamma h$ (x 10^{-25} ph s^{-1} cm^{-3} kpc)
Q_γ / Q_o
3.5
3.0
2.5
2.0
1.5
1.0
0.5
0
-0.5
-1.0
-1.5
-2.0
15
10
5
0
-5
-10
1.5
1.0
0.5
0
0.5
1.0
1.5
$R/R_\odot$

Fig. 3

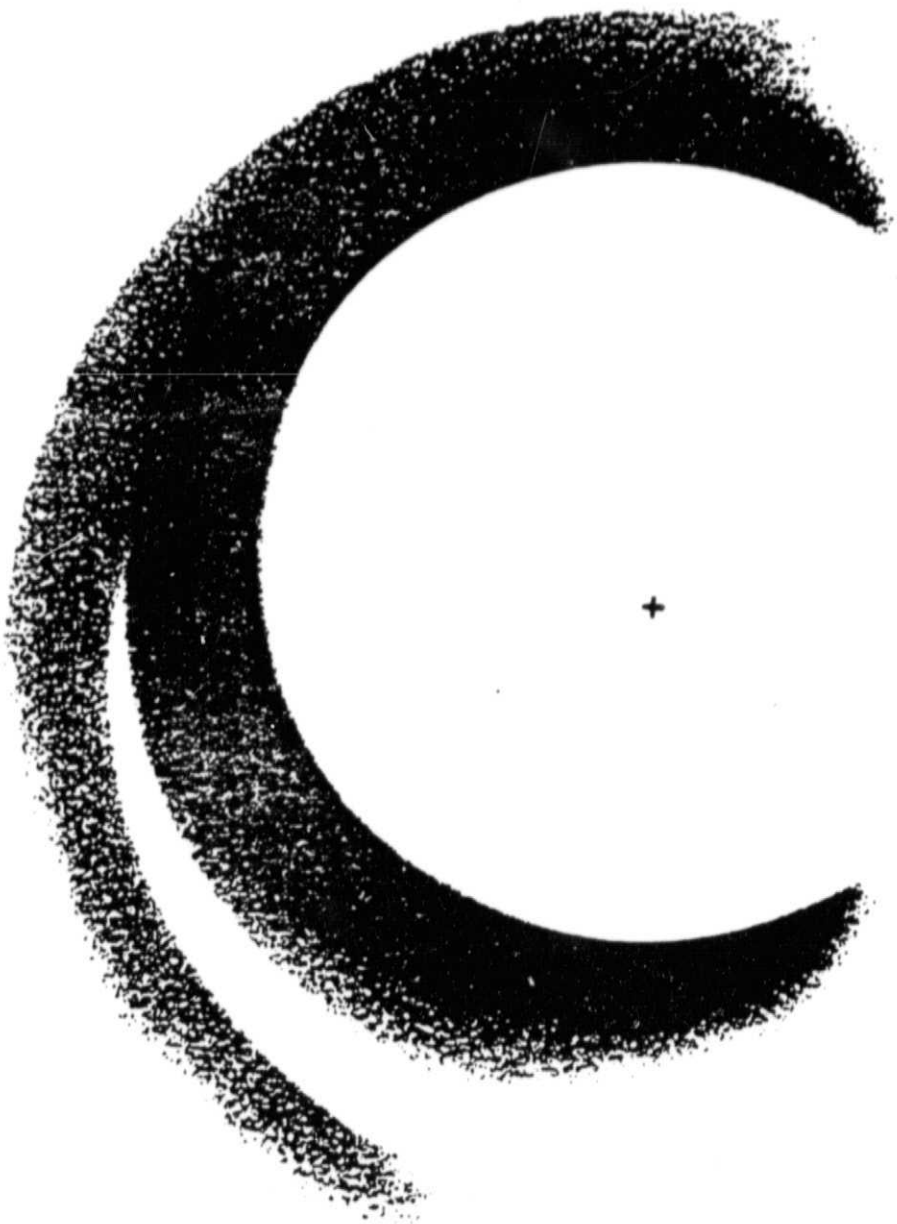

Fig. 4

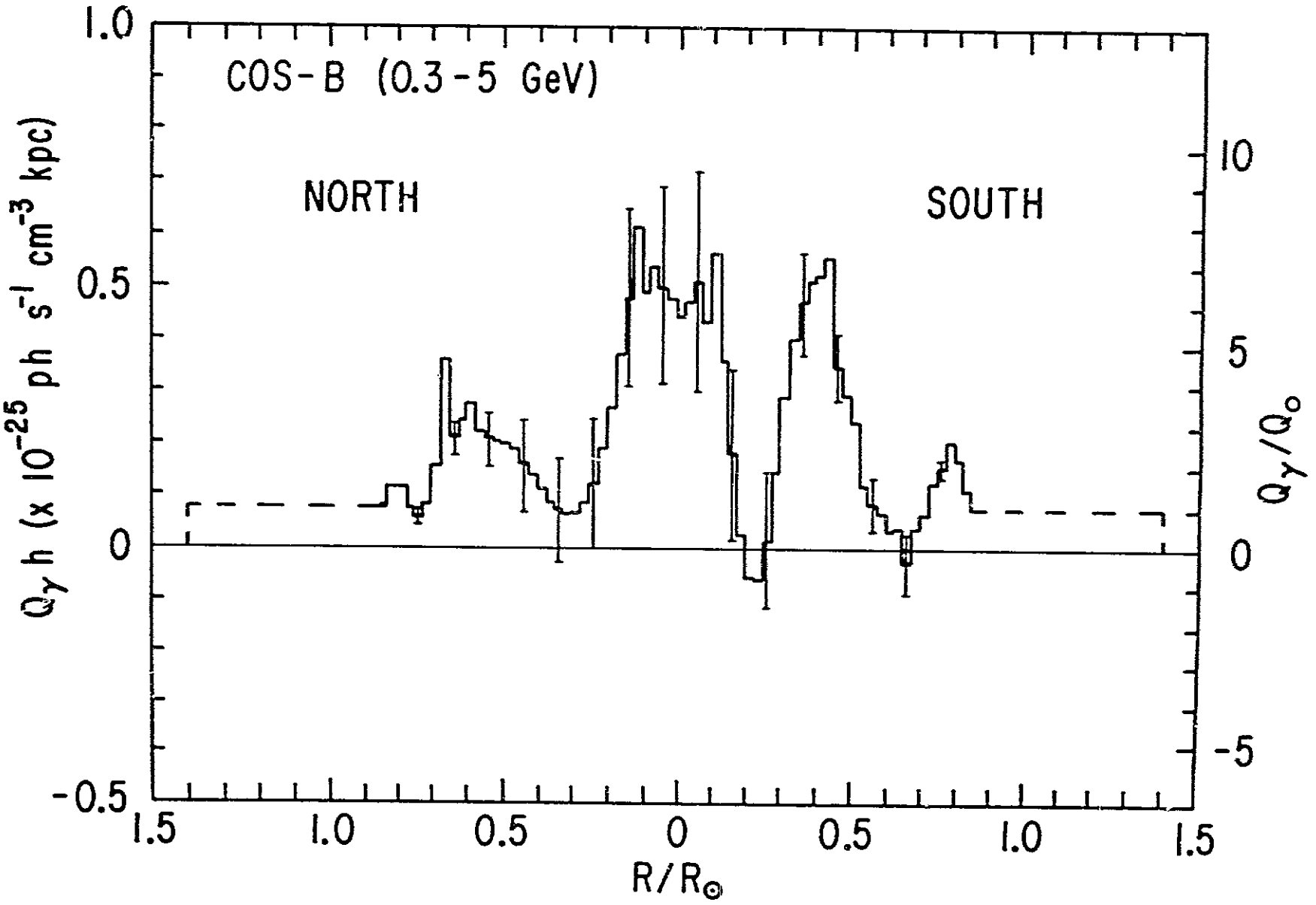
COS-B (0.3-5 GeV)
NORTH
SOUTH
$Q_\gamma h$ (x 10^{-25} ph s^{-1} cm^{-3} kpc)
Q_γ/Q_o
1.0
0.5
0
-0.5
10
5
0
-5
1.5
1.0
0.5
0
0.5
1.0
1.5
$R/R_\odot$

Fig. 5

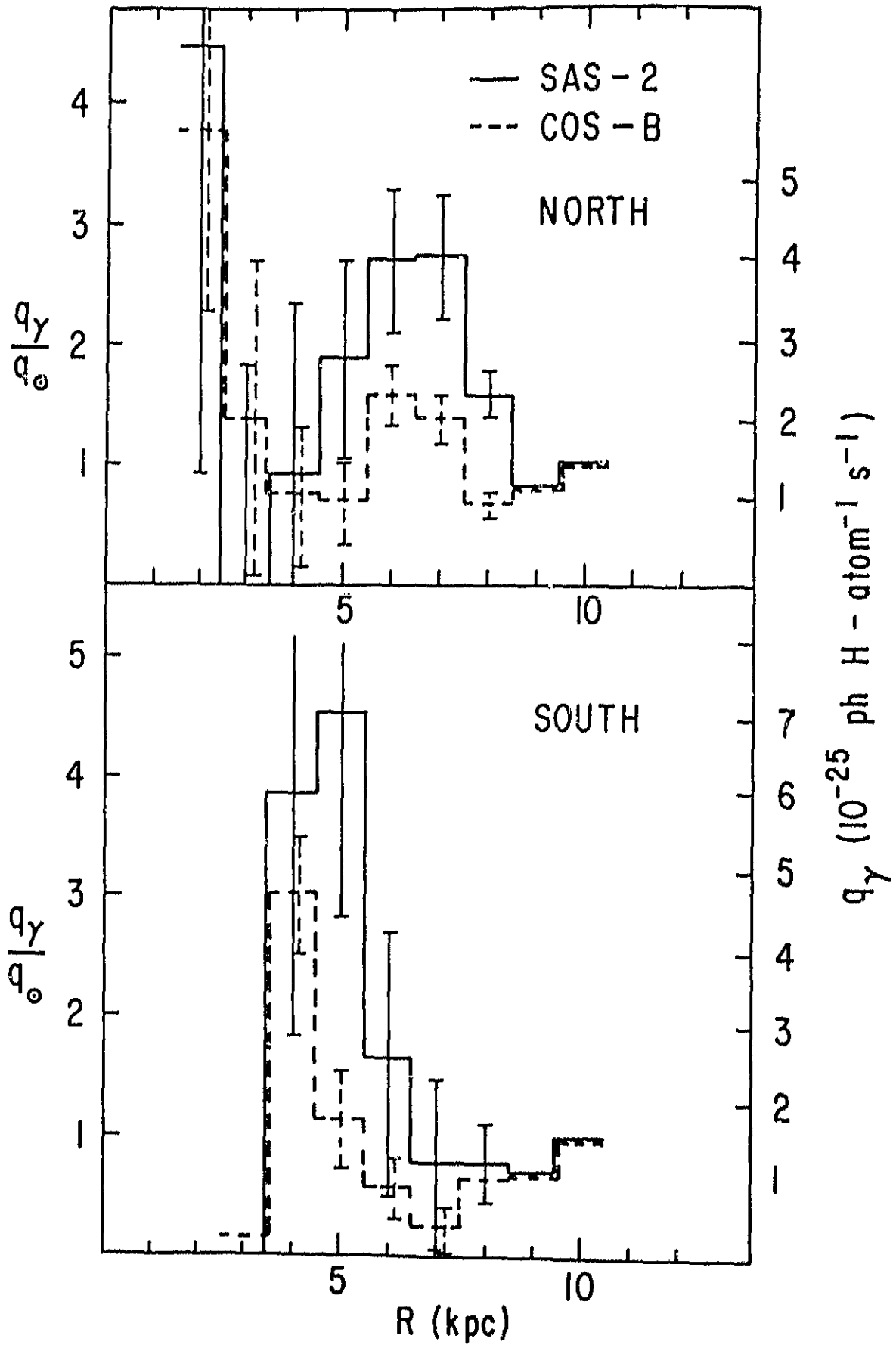
SAS - 2
COS - B
NORTH
SOUTH
$\frac{q_\gamma}{q_\odot}$
q_γ (10^{-25} ph H - atom^{-1} s^{-1})
R (kpc)
1
2
3
4
5
6
7
10

Fig. 6

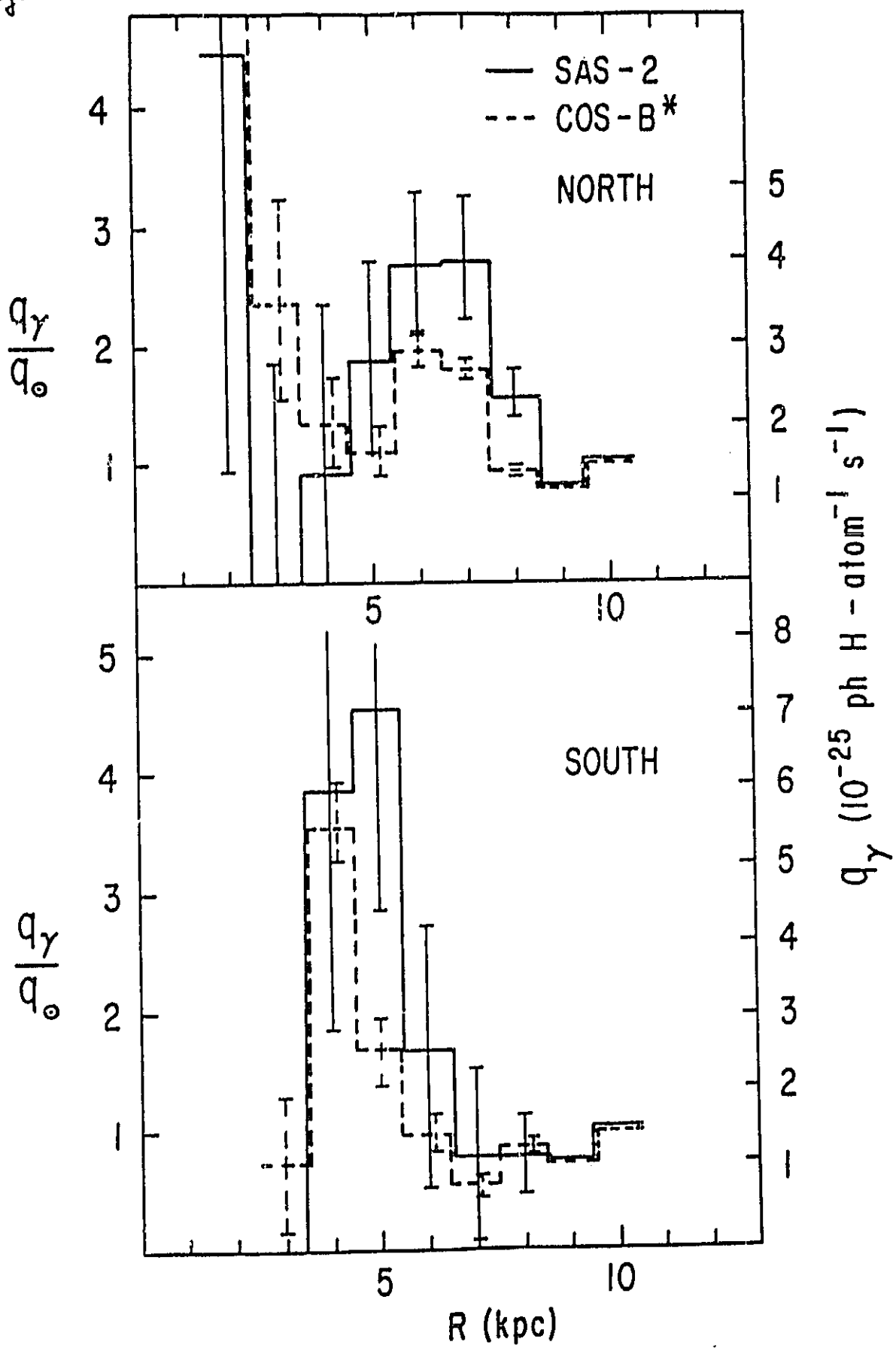
SAS-2
COS-B*
NORTH
SOUTH
$\frac{q_\gamma}{q_\odot}$
q_γ (10^{-25} ph H-atom^{-1} s^{-1})
R (kpc)

Fig. 7

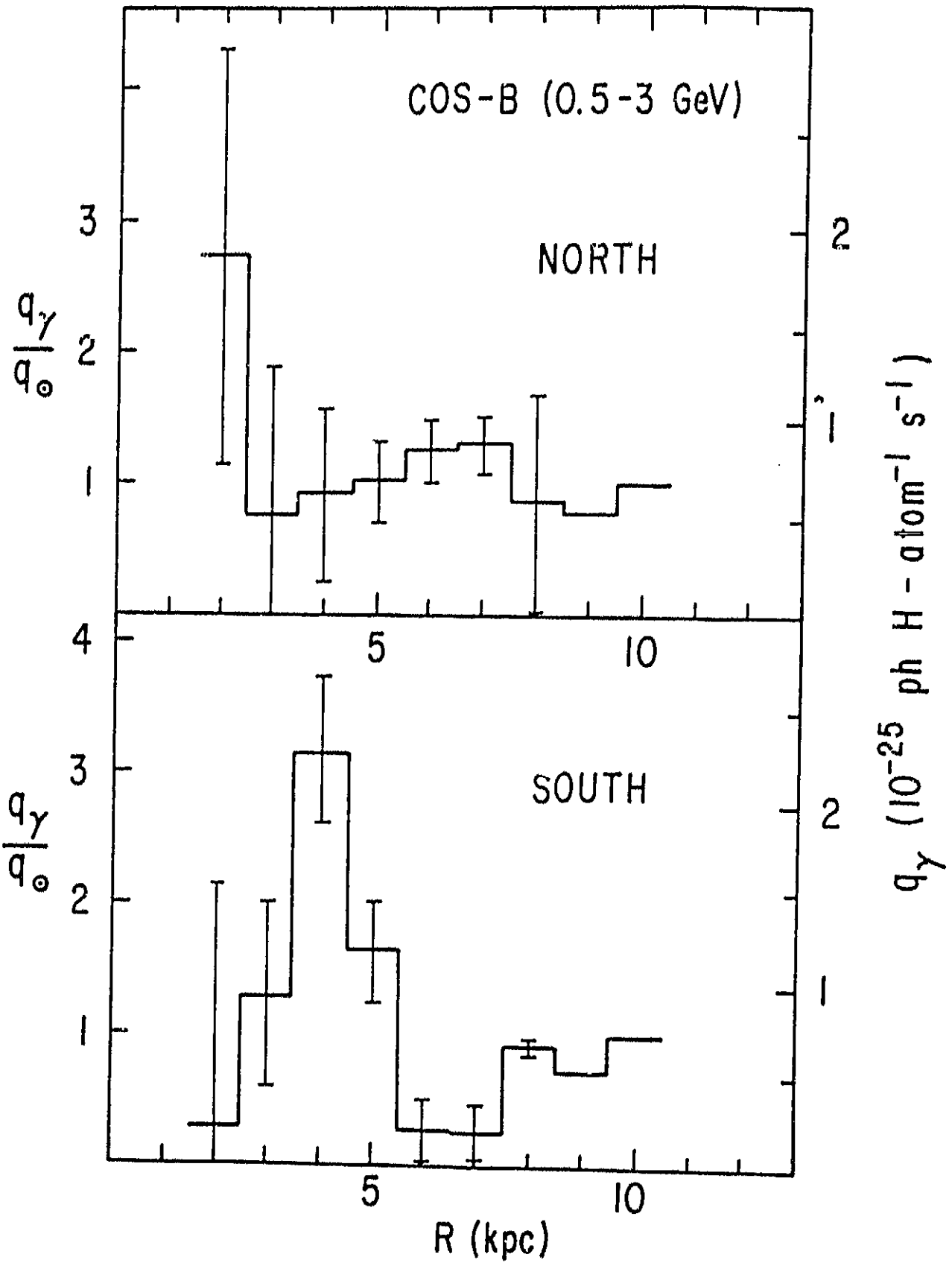
COS-B (0.5-3 GeV)
NORTH
SOUTH
$\frac{q_\gamma}{q_\odot}$
q_γ (10^{-25} ph H-atom^{-1} s^{-1})
R (kpc)
1
2
3
4
5
10